STABILIZING AND IMPROVING THE ACTIVE VIBRATION DAMPING BY A NEW S-Z MAPPING FOR DIGITAL CONTROL

Marcelo Ricardo Alves da Costa Tredinnick
PUC-RJ. Department of Electronic Engineering. Brazil
tredinnick@ele.puc-rio.br
Marcelo Lopes de Oliveira e Souza
INPE. Electronics and Simulation Laboratory. Brazil.
marcelo@dem.inpe.br

ABSTRACT

This paper presents an analytical and simulation study of the stabilization and improvement of the active vibration damping of a system modeled by a simple analog harmonic oscillator driven by discrete time control. Initially, this control is the Bilinear (or Tustin) s-z mapping equivalent of a continuous-time asymptotically stable Proportional plus Derivative (PD) control. It is tested with high values of the sampling period. It is shown that all classical mappings (Tustin, Schneider, etc.) tested may instabilize the system. To circumvent this, we propose and use a new (ST1) mapping that behaves better than the classical ones tested under the same conditions. We also model an active discrete control of a suspension of a vehicle, and compare the performance between the PD controllers designed by Bilinear and by the new (ST1) S-Z mappings, for this example.

1. Introduction.

Digital controls of analog plants, including vehicle suspensions, are becoming very common today due to their low price, extensive programming, logic and arithmetic capabilities, etc. Despite these advantages, their time sampling, amplitude quantization, and input, processing, and output delays are important disadvantages to be considered. They may become critical when the plant has oscillation modes that are above the Nyquist frequency (half of the sampling frequency), as happens in suspensions with some flexible modes. Then, a careful study of their consequences on that control and even on its stability must be done.

This paper presents an analytical and simulation study of the stabilization of an analog harmonic oscillator driven by discrete time controls. This control initially is the Tustin s-z mapping equivalent of a continuous-time asymptotically stable proportional plus derivative (PD) control. It is tested with high values to the sampling period. It is shown that all classical mappings (Tustin, Schneider, etc.) tested may instabilize the system. To circumvent this, we propose and use a new (ST1) mapping that behaves better than the classical ones tested under the same conditions.

2.The harmonic oscillator used

In this work we analyzed and simulated an (damped or undamped) harmonic oscillator given by:

$$m.\ddot{x}(t) + b.\dot{x}(t) + k.x(t) = u(t), \qquad y(t) = x(t) \quad \text{(Eq. 1)}$$

where $m \in (0;\infty)$, $b \in [0;m)$, $k \in (0;\infty)$, with analog transfer function given by:

$$G(s) \overset{\Delta}{=} \frac{Y(s)}{U(s)} = \frac{1}{k}.\frac{\omega_n^{\,2}}{s^2 + 2.\zeta.\omega_n.s + \omega_n^{\,2}} \quad \text{(Eq. 2)}$$

where $\omega_n = \sqrt{k/m} \in (0;\infty)$ is the non-damped natural angular frequency of this vibration mode, and $\zeta = b/m \in [0;1)$ is its damping ratio.

According to Franklin (1981), the zero-order hold (ZOH) equivalent of Eq. 2 may be calculated by:

$$G_{H0}(z) = (1 - z^{-1}).\mathscr{Z}\left\{ \mathcal{L}^{-1}\left\{\frac{G(s)}{s}\right\}\bigg|_{t=k.T_S} \right\} \qquad \text{(Eq.3)}$$

Applying Eq. 3 to Eq. 2 we have, after normalizing k=1:

$$G_{H0}(z)=\frac{z.\left[1-2e^{-\sigma T_S}.\cos(\omega_d T_S)-e^{-\sigma T_S}.\left(\frac{\sigma}{\omega_d}.\sin(\omega_d T_S)-\cos(\omega_d T_S)\right)\right]+e^{-2\sigma T_S}+e^{-\sigma T_S}.\left(\frac{\sigma}{\omega_d}.\sin(\omega_d T_S)-\cos(\omega_d T_S)\right)}{z^2-[2.e^{-\sigma T_S}.\cos(\omega_d T_S)]z+e^{-2\sigma T_S}}$$

(Eq. 4)

where T_S is the sampling period, $\sigma = \zeta.\omega_n \in (0;\omega_n)$ is the inverse of the decay time constant, $\omega_d = \omega_n.\sqrt{1-\zeta^2} \le \omega_n$ is the damped natural angular frequency. For an undamped harmonic oscillator ($\zeta = 0$), Equations 1, 2, and 4 may be reduced to Equations 5, 6, and 7, as follows:

$$m.\ddot{x}(t) + k.x(t) = u(t), \qquad y(t) = x(t) \qquad \text{(Eq. 5)}$$

$$G(s) \stackrel{\Delta}{=} \frac{Y(s)}{U(s)} = \frac{1}{k}.\frac{\omega_n^{\ 2}}{s^2 + \omega_n^{\ 2}} \qquad \text{(Eq. 6)}$$

$$G_{H0}(z) = [1 - \cos(\omega_n.T_S)].\frac{z+1}{z^2 - (2.\cos(\omega_n.T_S)).z + 1} \qquad \text{(Eq. 7)}$$

3. The Analog PD control

To simplify the analysis, we used an (stabilizing but noncausal) analog PD direct control (Figure 1), given by:

$$D(s) \stackrel{\Delta}{=} \frac{U(s)}{E(s)} = k_p + k_d.s \qquad \text{(Eq. 8)}$$

where k_p e k_d are the control gains for the proportional and derivative actions, respectively, and e(t) = r(t) - x(t).

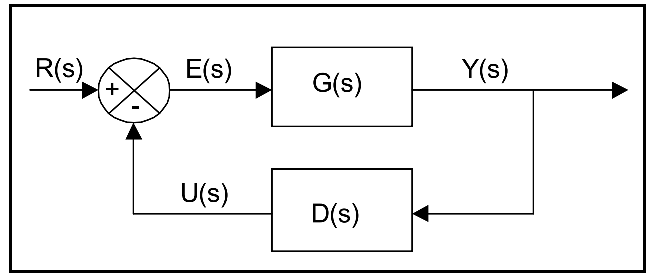

Fig. 1. Block diagram of the closed-loop analog system.

4. The Discrete-time PD control

We also used the correspondent discrete-time PD direct control D(z) (Figure 2) given by the next sections.

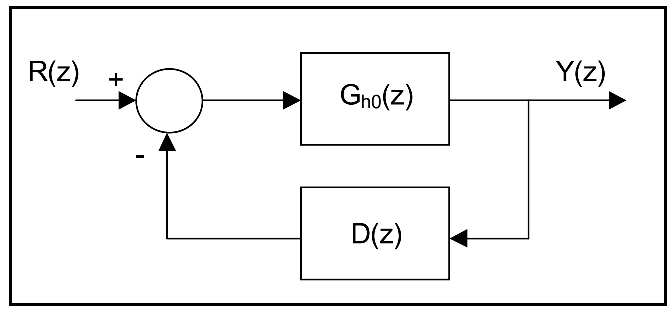

Fig. 2. Block diagram of the closed-loop discrete time system.

4.1. Discrete PD control designed by Tustin rule.

The Tustin s-z mapping is:

$$s \sim \frac{2}{T_S}.\frac{z-1}{z+1} \qquad \text{(Eq.9)}$$

Substituting Eq. 9 in Eq. 8 we have:

$$D(z) = k_p + k_d.\frac{2}{T_S}.\frac{z-1}{z+1}\text{, or} \qquad \text{(Eq.10)}$$

$$D(z) = \left(k_p + \frac{2.k_d}{T_S}\right).\frac{z + \left(\frac{k_p.T_S - 2.k_d}{k_p.T_S + 2.k_d}\right)}{z+1} \qquad \text{(Eq.11)}$$

4.2. Discrete PD control designed by Schneider rule 1.

The Schneider s-z mapping 1 is:

$$s \sim \frac{E(z)}{U(z)} = \frac{12}{T_S} \cdot \frac{z.(z-1)}{5z^2 + 8z - 1} \quad \text{(Eq.12)}$$

Substituting Eq. 12 in Eq. 8 we have:

$$D(z) = \frac{\left(5 \cdot k_p + 12 \cdot \frac{k_d}{T_S}\right).z^2 + \left(8 \cdot k_p - 12 \cdot \frac{k_d}{T_S}\right).z - k_p}{5.z^2 + 8.z - 1} \quad \text{(Eq.13)}$$

5. PD control of an harmonic oscillator

The harmonic oscillator control is interpreted here as a kind of active vibrational control. The idea here is: initially, to study an active control of an harmonic oscillator; and later, to extend it to the attitude control of a model of a system with some flexible modes, as done in Tredinnick (1999a, b), considering the appendage vibrations as the principal disturbances on the satellite attitude.

5.1. Analog PD control of an analog harmonic oscillator

For the totally analog case we specified m, b, k, and transients with: peak time $t_p \cong 0{,}6$ segundos; settling time $t_s \cong 5$ segundos; overshoot $M_P \cong 0{,}15$ Nm, which gave k_p, k_d.

5.2 Tustin PD control of a ZOH equivalent of an harmonic oscillator.

The closed-loop transfer function H(z) of the system shown in Figure 2 (without canceling the pole of D(z) with the zero of $G_{h0}(z)$) is given by:

$$H(z) = \frac{Y(z)}{R(z)} = \frac{\dfrac{[1-\cos(\omega_n.T_S)].(z+1)}{z^2 - 2.\cos(\omega_n.T_S).z + 1}}{1 + \dfrac{[1-\cos(\omega_n.T_S)].(z+1)}{z^2 - 2.\cos(\omega_n.T_S).z + 1} \cdot \dfrac{\left(k_p + 2.k_d/T_S\right).\left(z + \left(\dfrac{k_p.T_S - 2.k_d}{k_p.T_S + 2.k_d}\right)\right)}{(z+1)}} \quad \text{(Eq. 14)}$$

or, after rearranging:

$$H(z) = [1-\cos(\omega_n.T_S)].\frac{z^2 + 2.z + 1}{z^3 + \left[1 - 2.\cos(\omega_n.T_S) + \left(k_p + 2k_d/T_S\right).[1-\cos(\omega_n.T_S)]\right].z^2 + \ldots}$$

$$\ldots \left[1 - 2.\cos(\omega_n.T_S) + \left(k_p + 2k_d/T_S\right).[1-\cos(\omega_n.T_S)].\left(\frac{k_p.T_S - 2.k_d}{k_p.T_S + 2.k_d} + 1\right)\right].z + 1 + \ldots$$

$$\ldots + \left(k_p + 2k_d/T_S\right).[1-\cos(\omega_n.T_S)].\left(\frac{k_p.T_S - 2.k_d}{k_p.T_S + 2.k_d}\right) \quad \text{(Eq.15)}$$

If we cancel the pole of D(z) with the zero of $G_{h0}(z)$ in the denominator of the equation, Eqs. 14 and 15 become respectively Eqs. 16 and 17 below:

$$H(z) = [1-\cos(\omega_n.T_S)].\frac{z+1}{z^2 + \left[\left(k_p + 2k_d/T_S\right).[1-\cos(\omega_n.T_S)] - 2.\cos(\omega_n.T_S)\right].z + 1 + \left(k_p + 2k_d/T_S\right). \ldots}$$

$$\ldots .[1-\cos(\omega_n.T_S)].\left(\frac{k_p.T_S - 2.k_d}{k_p.T_S + 2.k_d}\right) \quad \text{Eq.16)}$$

$$H(z)=\left[1-\cos(\omega_n.T_S)\right].\frac{z+1}{z^2+\left[\left(k_p+{}^{2k_d}\!/_{T_S}\right).\left[1-\cos(\omega_n.T_S)\right]-2.\cos(\omega_n.T_S)\right].z+\ldots} \ldots$$

(Eq.17)

$$\ldots \quad \overline{+1+\left(k_p-{}^{2k_d}\!/_{T_S}\right).\left[1-\cos(\omega_n.T_S)\right]}$$

Eqs. 16 and 17 have the following characteristic equation:

$$1+\left(k_p+{}^{2k_d}\!/_{T_S}\right).\left[1-\cos(\omega_n.T_S)\right].\frac{z+\left(\dfrac{k_p.T_S-2.k_d}{k_p.T_S+2.k_d}\right)}{z^2-[2.\cos(\omega_n.T_S)].z+1}=0 \qquad \text{(Eq.18)}$$

or, after rearranging:

$$z^2+\left[\left(k_p+{}^{2k_d}\!/_{T_S}\right).\left[1-\cos(\omega_n.T_S)\right]-2.\cos(\omega_n.T_S)\right].z+1+\left(k_p-{}^{2k_d}\!/_{T_S}\right).\left[1-\cos(\omega_n.T_S)\right]=0 \qquad \text{(Eq.19)}$$

$$z^2+\left[\left(\frac{k_p.T_S+2k_d}{T_S}\right).\left[1-\cos(\omega_n.T_S)\right]-2.\cos(\omega_n.T_S)\right].z+1+\left(\frac{k_p.T_S-2k_d}{T_S}\right).\left[1-\cos(\omega_n.T_S)\right]=0 \qquad \text{(Eq. 20)}$$

6. Analysis and simulations with classical methods.

6.1. Analog PD control of an analog harmonic oscillator.

Figure 3 shows the root locus in the s-plane of the analog system of Figure 1 with the G(s) of Eq.2 and the D(s) of Eq. 8 varing k_p/k_d. Figure 4 shows its unit impulse response.

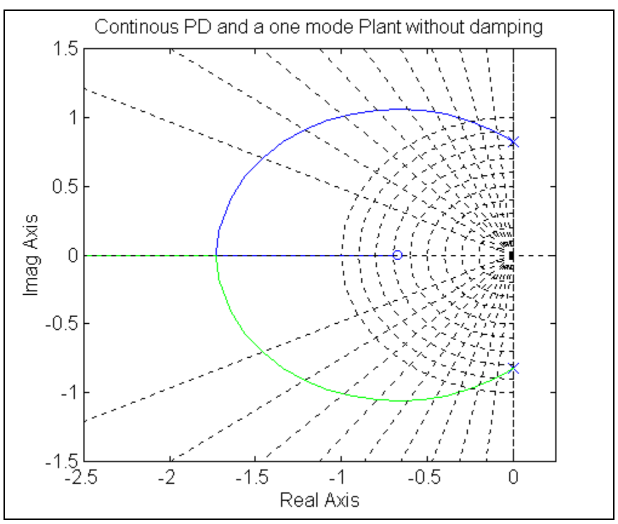

Fig. 3. Root-locus for G(s) of Eq.2 and D(s) of Eq. 8 varing k_p/k_d.

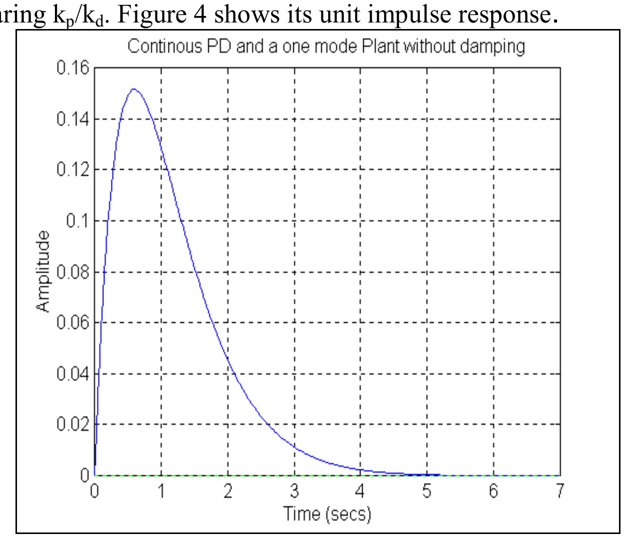

Fig. 4. Unit impulse response for G(s) of Eq.2 and D(s) of Eq.8.

6.2. Tustin PD control of the ZOH equivalent of an undamped harmonic oscillator

Figure 5 shows the root locus in the z-plane of the discrete-time system of Figure 2, with G(z) of Eq. 7 and the D(z) of Eq. 10 for Ts = 0,1 s varing k_p/k_d. Figure 6 shows its unit pulse response.

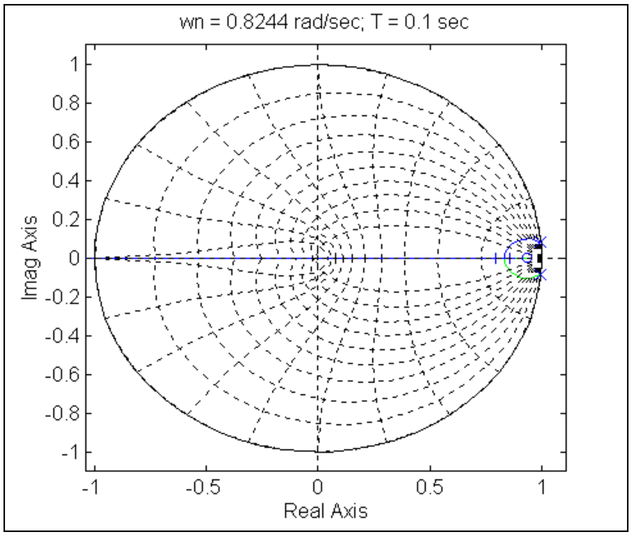

Fig. 5. Root-locus for G(z) of Eq. 7, D(z) of Eq. 10 and T_S = 0,1 s varing k_p/k_d.

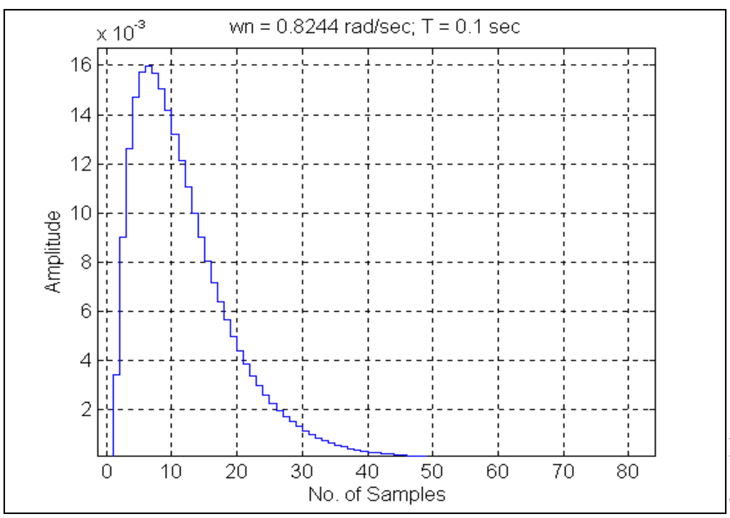

Fig. 6. Unit pulse response for G(z) of Eq. 7, D(z) of Eq. 10 and T_S = 0,1 s.

Figure 7 shows the root locus in the z-plane of the discrete-time system of Figure 2, with G(z) of Eq. 7 and the D(z) of Eq. 10 for Ts = 1,6 s varing k_p/k_d. Figure 8 shows its unit pulse response.

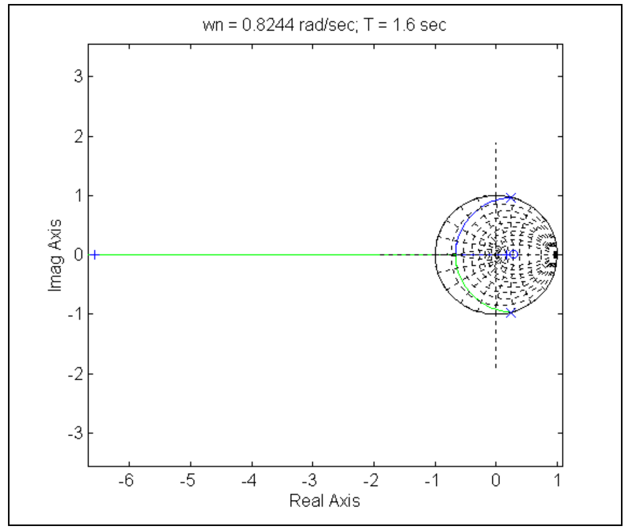

Fig. 7. Root-locus for G(z) of Eq. 7, D(z) of Eq. 10 and T_S = 1,6 s varing k_p/k_d.

In Figure 7 we may observe the pole outside the unit circle that unstabilize Figure 8.

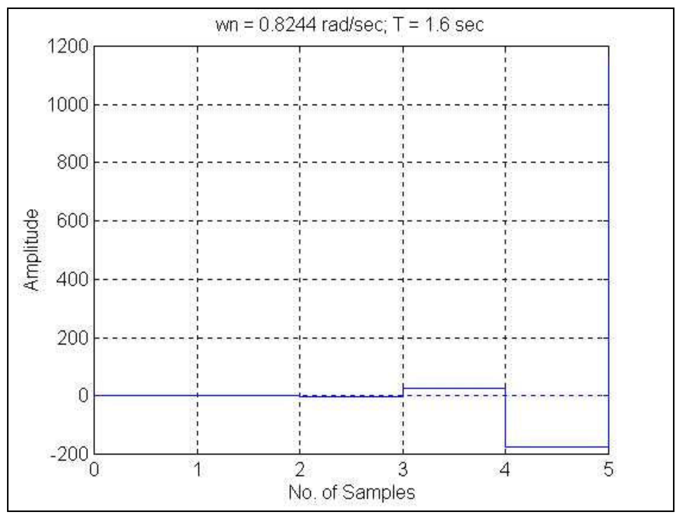

Fig. 8. Unit pulse response for G(z) of Eq. 7, D(z) of Eq. 10 and T_S = 1,6 s.

6.3. Tustin PD control of the ZOH equivalent of a damped harmonic oscillator

Figure 9 shows the root locus in the z-plane of the discrete-time system of Figure 2 with G(z) of Eq.7, with damping ratio

$\zeta = 0.1$, and the D(z) of Eq. 10 for Ts = 0,1 s. Figure 10 shows its unit pulse response.

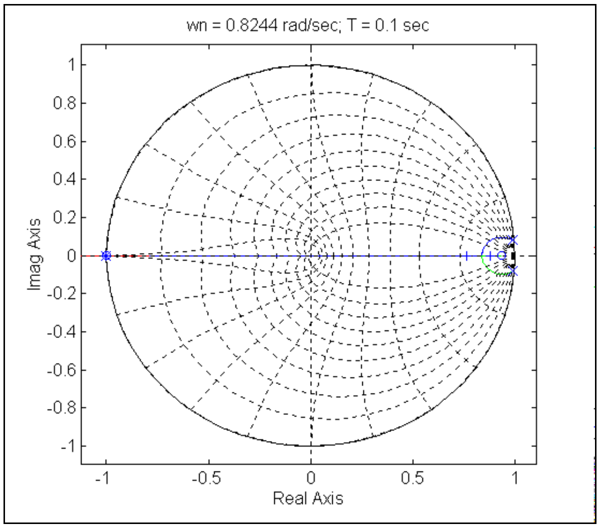

Fig. 9. Root-locus for G(z) of Eq.7, $\zeta = 0.1$, D(z) of Eq. 10 and $T_S = 0,1$ s.

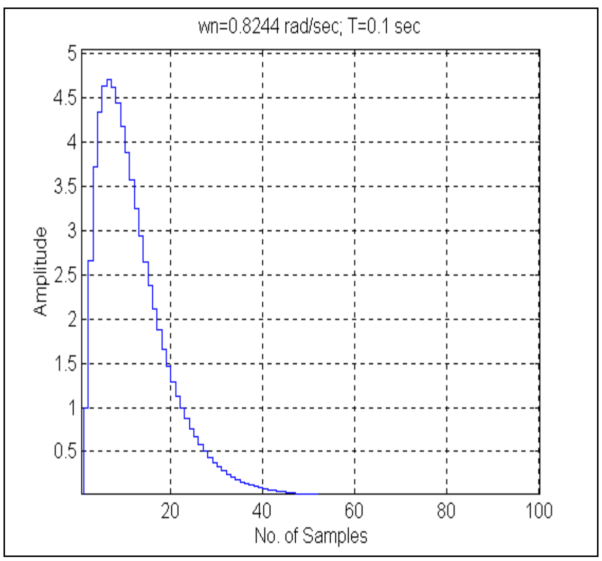

Fig. 10. Unit pulse response for G(z) of Eq.7, $\zeta = 0.1$, D(z) of Eq. 10, $T_S = 0,1$ s.

6.4 Schneider PD control of the ZOH equivalent of a damped harmonic oscillator

Figure 11 shows the root locus in the z-plane of the discrete-time system of Figure 2, with G(z) of Eq. 4, D(z) of Eq. 13, ζ =6, Ts = 1,6 s varing k_p/k_d. Figure 12 shows its unit pulse response.

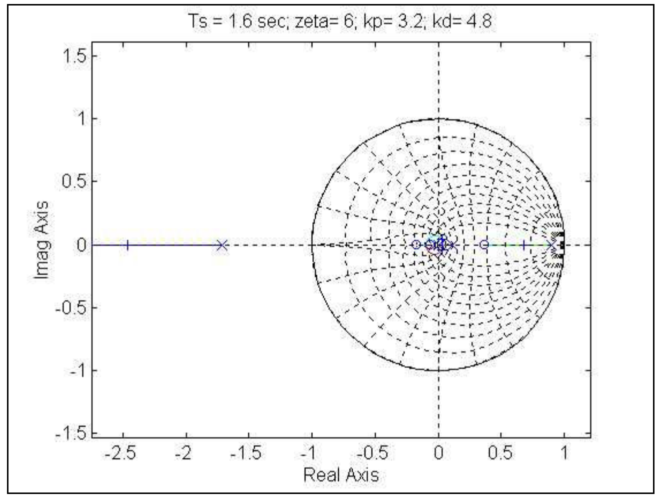

Fig. 11. Root-locus for G(z) of Eq. 4, D(z) of Eq. 13, ζ =6, Ts = 1,6 s varing k_p/k_d.

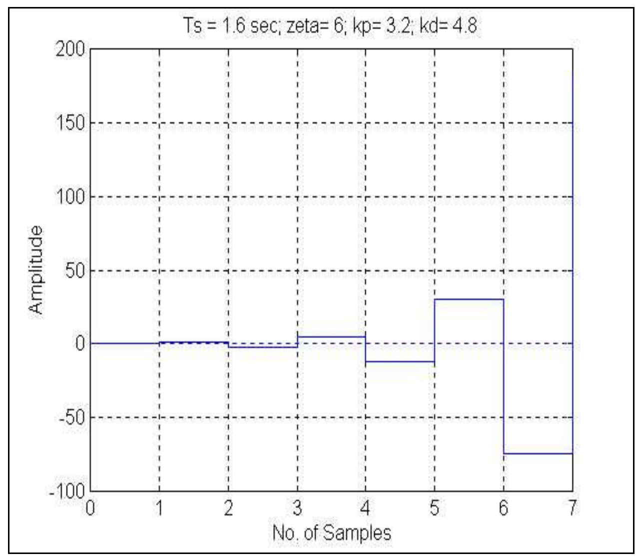

Fig. 12. Unit pulse response for G(z) of Eq. 4, D(z) of Eq. 13, ζ =6, Ts = 1,6 s.

By Schneider rule with $k_p = 3.2$ e $k_d = 4.8$, $T_S = 1,6$ s we still have instability and even with $\zeta = 120$, as shown in Figures 13 and 14.

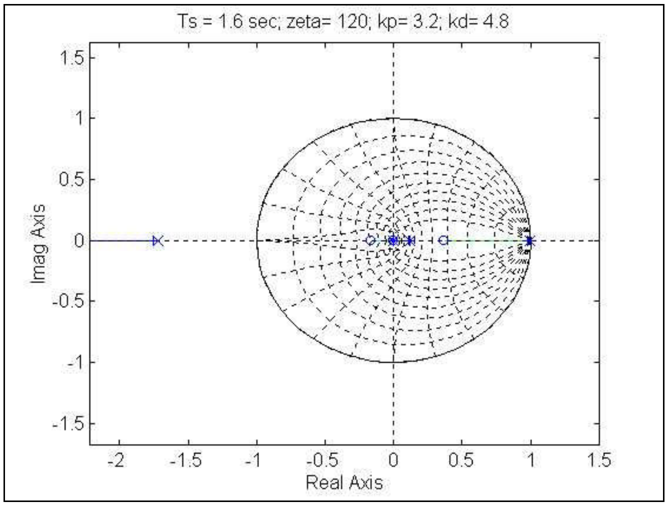

Fig. 13. Root-locus for G(z) of Eq. 4, D(z) of Eq. 13, ζ =6, Ts = 1,6 s varing k_p/k_d.

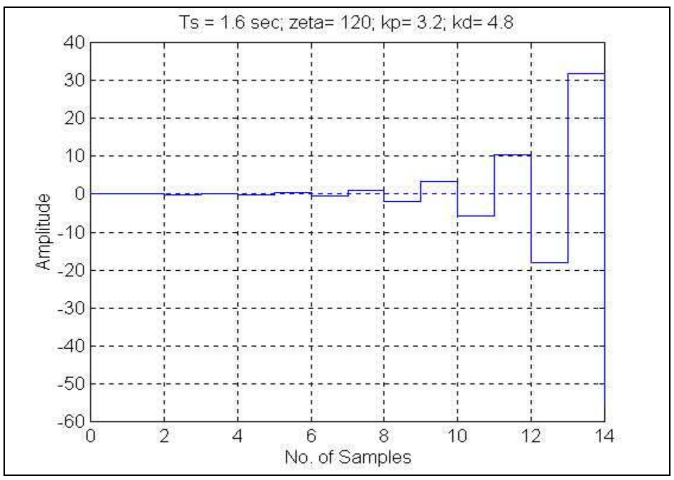

Fig. 14. Unit pulse response for G(z) of Eq. 4, D(z) of Eq. 13, ζ =6, Ts = 1,6 s.

By Schneider rule with k_p = 3.2 e k_d = 4.8, T_S = 1,6 s we still have instability and even with ζ = 0, as shown in Figures 15 and 16.

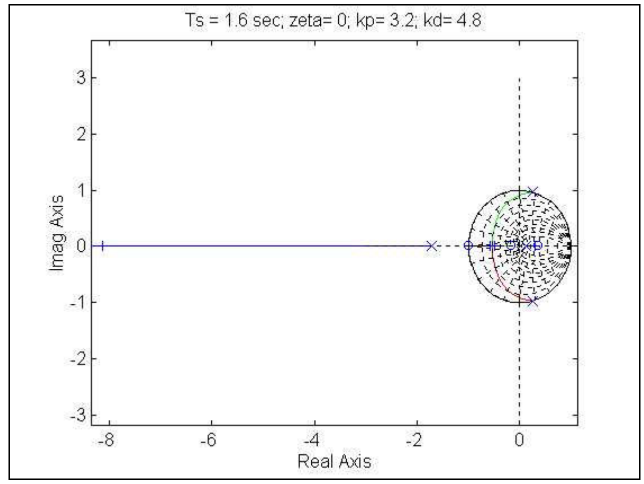

Fig. 15. Root-locus for G(z) of Eq. 4, D(z) of Eq. 13, ζ =0, Ts = 1,6 s varing k_p/k_d.

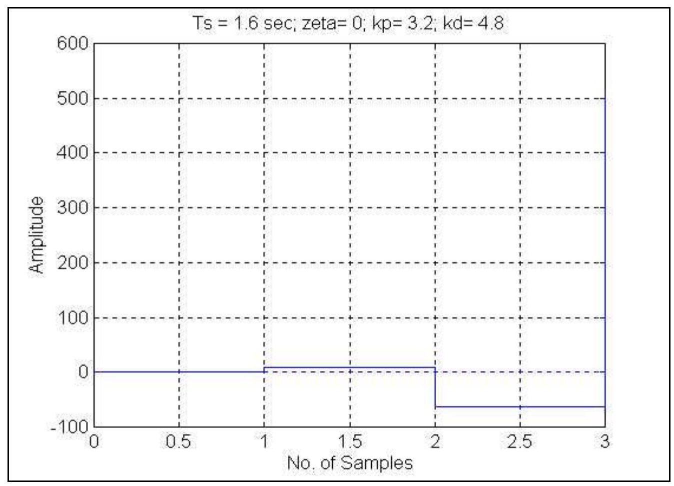

Fig. 16. Unit pulse response for G(z) of Eq. 4, D(z) of Eq. 13, ζ =0, Ts = 1,6 s.

Figures 11 - 16, show that all cases controlled by Schneider PD rule are unstable.

6.4.1 Schneider lead control of the ZOH equivalent of a damped harmonic oscillator

The Schneider rule 1 (Eq.12) cannot be used in the PD controller (Eq.8) design because it presents a pole outside the unit circle. as hinted above and shown in Tredinnick(1999).
Figure 17 shows the discrete root-locus for $G_{h0}(z)$ = 1, with D(z) of Eq. 13 with kp = 0, and Ts= 1,6s, having: a) a (stable) pole inside the unit circle at z_1 = 0.116; and b) a (unstable) pole outside the unit circle at z_2 = -1.716. This unstabilizes derivative actions when designed by Schneider rule 1.

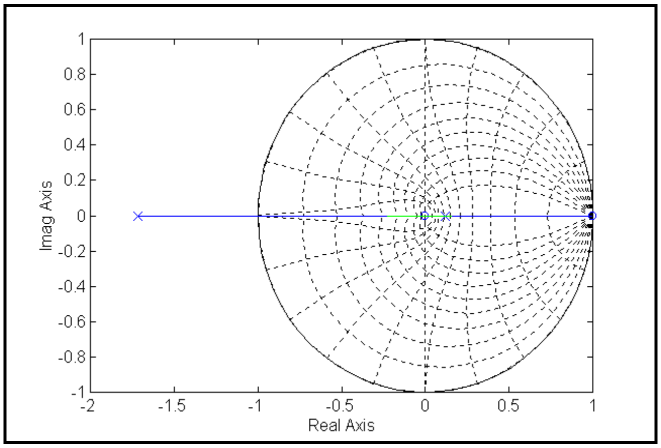

Fig. 17. Root locus for $G_{h0}(z) = 1$, with D(z) of Eq. 13 with kp = 0, and Ts= 1,6s.

7. Proposal of new-s-z mapping.

The limitations of the classical methods presented so far in preserving the stability for high gains and high sampling periods suggested us to propose new s-z mappings. This begun in the work of Tredinnick (1999a, b) through the difference equation:

$$e_k = \frac{2}{T_s}.\nabla u_k - \xi.e_{k-1} \qquad \text{(Eq. 21)}$$

Applying the z-transform (Franklin, 1981) on it we have the new s-z mapping 1:

$$s \sim \frac{2}{T_s}.\frac{z-1}{z+\xi} \qquad ;0<\xi<1 \qquad \text{(Eq. 22)}$$

which shifts the pole from z = -1 in the Tustin rule to z' = -ξ, 0 ≤ ξ ≤ 1. This avoids or retards the instabilization in closed loop systems, by using ξ as a new design parameter (besides the control gains and the sampling period). The new rule 1 becomes: the Tustin rule for ξ = 1; and the backward mapping for ξ = 0. Its inverse is given by:

$$s = \frac{2}{T_S}.\frac{z-1}{z+\xi} \quad \Rightarrow \quad z = \frac{2+s.T_S.\xi}{2-s.T_S} \qquad (-1 \le \xi \le 1) \quad \text{(Eq. 23)}$$

The new rule also maps the left half s plane into a circle with center between z = ½ and z = 0 and radius between ¼ and 1, respectively, always inside the unit circle in plane z as proved in Tredinnick(1999).

7.1. New-rule designing the PD control

A PD controller designed by new-rule 1 is given by:

$$D(z) = PD_{\ control} = \left(k_p + \frac{2.k_d}{T_S}\right).\frac{z + \left(\dfrac{k_p.T_S.\xi - 2.k_d}{k_p.T_S + 2.k_d}\right)}{z+\xi} \qquad \text{(Eq. 24)}$$

8. Simulations with the new-rule.

8.1. New rule 1 PD control of a ZOH equivalent of a damped harmonic oscillator.

Figure 18 shows the root locus in the z-plane of the discrete-time system of Figure 2, with G(z) of Eq. 4 with damping ratio ζ = 6, and the D(z) of Eq. 44 for Ts = 1,6 s varing k_p/k_d. Figure 19 shows its (asymptotically stable) unit pulse response for k_p = 3, k_d = 4.8, T_S = 1.6 s, ξ = 0.2:

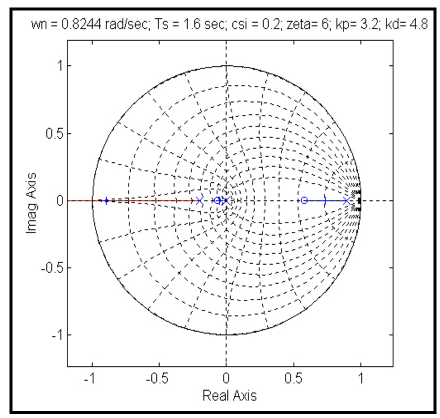

Fig.18. Root-locus for G(z) of Eq. 4, D(z) of Eq.44, ζ =6, Ts = 1,6 s, ξ = 0.2 varing k_p/k_d.

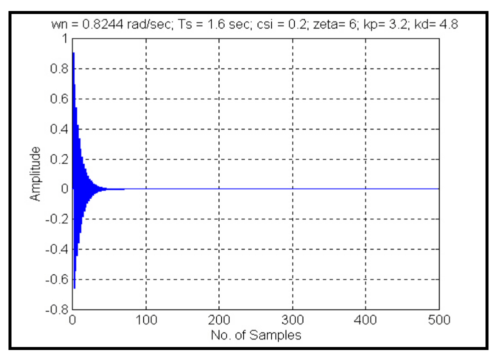

Fig.19. Unit pulse response for G(z) of Eq. 4, D(z) of Eq. 44, ζ =6, Ts = 1,6 s, ξ = 0.2, k_p = 3, k_d = 4.8,.

9. Improving the performance of the active suspension of a vehicle control of by a new s-z mapping

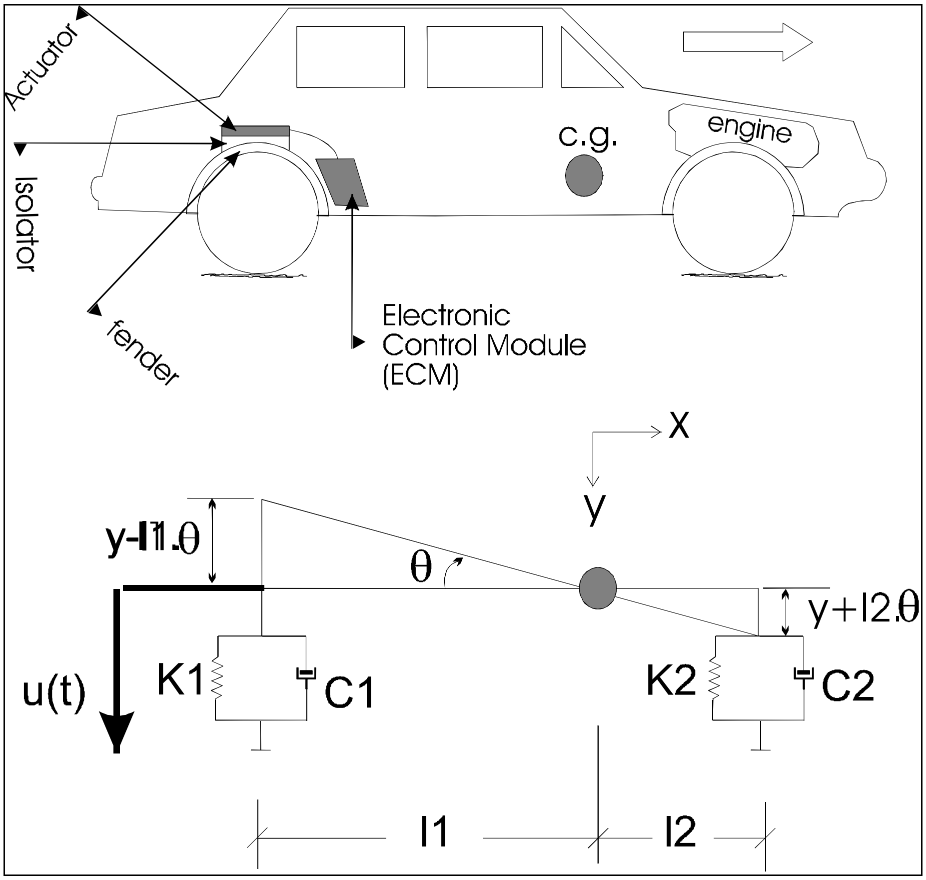

Fig.20. Active Digital Suspension System

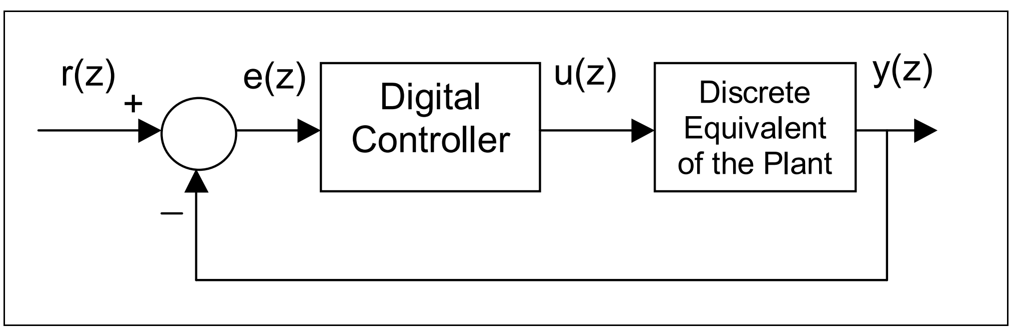

Fig. 21. Discrete-time active control of the vehicle suspension.

The vertical and rotational equations of motion in Fig. 20 are:

$$m.\ddot{y} = -c_1.\left(\dot{y} - l_1.\dot{\theta}\right) - c_2.\left(\dot{y} + l_2.\dot{\theta}\right) - k_1.(y - l_1.\theta) - k_2.(y + l_2.\theta) + u(t) \qquad \text{(Eq.25)}$$

$$J.\ddot{\theta} = c_1.l_1.\left(\dot{y} - l_1.\dot{\theta}\right) - c_2.l_2.\left(\dot{y} + l_2.\dot{\theta}\right) + k_1.l_1.(y - l_1.\theta) - k_2.l_2.(y + l_2.\theta) + u(t).l_1$$

where m and J are the mass and the polar moment of inertia of the vehicle, k_1, k_2 are the elastic constants of the springs, c_1, c_2 are the damping coefficients of the piston, with values:

m = 1800 kg;
J = 630 kg.m^2;
$c_1 = c_2 = 0.2$;
$k_1 = k_2 = 0.2$;
$l_1 = 1.3$ m;
$l_2 = 0.5$ m;

Doing now:

$$\underline{p} = \begin{pmatrix} y(t) \\ \theta(t) \end{pmatrix} \quad \text{(Eq.26)}$$

we have,

$$\begin{pmatrix} m & 0 \\ 0 & J \end{pmatrix}.\ddot{\underline{p}}(t) + \begin{pmatrix} c_1 + c_2 & l_2.c_2 - l_1.c_1 \\ l_2.c_2 - l_1.c_1 & l_2^2.c_2 + l_1^2.c_1 \end{pmatrix}.\dot{\underline{p}}(t) + \begin{pmatrix} k_1 + k_2 & l_2.k_2 - l_1.k_1 \\ l_2.k_2 - l_1.k_1 & l_2^2.k_2 + l_1^2.k_1 \end{pmatrix}.\underline{p}(t) = \begin{pmatrix} 1 \\ l_1 \end{pmatrix}.u(t)$$

$$\begin{pmatrix} 1800 & 0 \\ 0 & 630 \end{pmatrix}.\ddot{\underline{p}}(t) + \begin{pmatrix} 0.4 & -0.16 \\ -0.16 & 0.38 \end{pmatrix}.\dot{\underline{p}}(t) + \begin{pmatrix} 0.4 & -0.16 \\ -0.16 & 0.38 \end{pmatrix}.\underline{p}(t) = \begin{pmatrix} 1 \\ 1.3 \end{pmatrix}.u(t)$$

$$M.\ddot{\underline{p}}(t) + D.\dot{\underline{p}}(t) + K.\underline{p}(t) = \underline{F}(t) \quad \text{(Eq.27)}$$

We may calculate the vibration modes of this system doing:

$$M^{-1/2} = \begin{pmatrix} 0.02357 & 0 \\ 0 & 0.03984 \end{pmatrix}$$

$$\tilde{D} = M^{-1/2}.D.M^{-1/2}$$

$$\tilde{K} = M^{-1/2}.K.M^{-1/2}$$

The matrix P is the matrix of the eigenvectors of $\tilde{K}$:

$$P = \begin{pmatrix} 0.9448 & -0.3278 \\ 0.3278 & 0.9448 \end{pmatrix}$$

we have, finally:

$$\Lambda = P^T.\tilde{K}.P = diag(\omega_1^2, \omega_2^2) = diag(0.1701, 0.6553)$$

where we have the natural modes of vibration as:

$$\omega_1 = 0.4124 \text{ rad/s}$$

$$\omega_2 = 0.8095 \text{ rad/s}$$

Considering the damping, we have:

$$\Xi = P^T.\tilde{D}.P = diag(2.\zeta_1.\omega_1, 2.\zeta_2.\omega_2) = diag(0.1701, 0.6553)$$

Given the damping ratios of the modes as

$$\zeta_1 = 0.2062$$

$$\zeta_2 = 0.4047$$

and, the damped modes are:

$$\omega_{d1} = \omega_1.\sqrt{1 - \zeta_1^2} = 0.403537 \text{ rad/s}$$

$$\omega_{d2} = \omega_2.\sqrt{1 - \zeta_2^2} = 0.740247 \text{ rad/s}$$

Writing in the space of states equation:

$$\underline{x}(t) = \begin{pmatrix} y(t) \\ \theta(t) \\ \dot{y}(t) \\ \dot{\theta}(t) \end{pmatrix}$$

$$\dot{\underline{x}}(t) = A.\underline{x(t)} + B.u(t)$$

where,

$$A = \begin{pmatrix} 0 & 0 & 1 & 0 \\ 0 & 0 & 0 & 1 \\ 0.0002 & -0.0001 & 0.0002 & -0.0001 \\ -0.0002 & 0.0004 & -0.0002 & 0.0006 \end{pmatrix}$$

$$B = \begin{pmatrix} 0 \\ 0 \\ 1 \\ 1.3 \end{pmatrix}$$

Supposing that only the vertical position is observed, we have:

$$C = \begin{pmatrix} 1 & 0 & 0 & 0 \end{pmatrix}$$

Finally, the analog transfer function G(s) is:

$$G(s) = C.[I.s - A]^{-1}.B$$

$$G(s) = \frac{s^2 - 0.0006788.s - 0.0005359}{s^4 - 0.0007938.s^3 - 0.00065083.s^2 + 0.0000001875.s + 0.00000007665} \qquad \text{(Eq.28)}$$

The Zero-Order Hold discrete-time equivalent of G(s), is given by:

$$G_{HO}(z) = (1 - z^{-1}).\mathcal{Z}\left\{ \mathcal{L}^{-1}\left\{\frac{G(s)}{s}\right\}\right\}$$

$$G_{HO}(z) = 0.5\ \frac{z^3 - z^2 - z + 1}{z^4 - 4.001445.z^3 + 6.00368.z^2 - 4.003.z + 1.00079}$$

(Eq.29)

Using a sampling period of T_S = 1 second, we do not have the aliasing fenomenon. This simulation is only to compare the performance between the PD controller designed by Tustin and ST1 rules without the aliasing fenomenon. A more realistic case must consider the digital control with an analog plant.

As we may see in Tredinnick (1999a), the PD controller designed by Bilinear rule is given by:

$$O(z) = \left(k_p + \frac{2.k_d}{T_S}\right).\frac{z + \left(\dfrac{k_p.T_S - 2.k_d}{k_p.T_S + 2.k_d}\right)}{z + 1} \qquad \text{(Eq.30)}$$

and the PD controller designed by ST1 rule is given by:

$$O(z) = \left(k_p + \frac{2.k_d}{T_S}\right).\frac{z + \left(\dfrac{k_p.T_S.\xi - 2.k_d}{k_p.T_S + 2.k_d}\right)}{z + \xi} \qquad \text{(Eq.31)}$$

where the control gains are:

$k_p = 0.01$;

$k_d = 0.10$;

The parameter $\xi = -0.15$.

The following figures shown that the ST1 rule presented as a better kind of design in comparison with the Bilinear method.

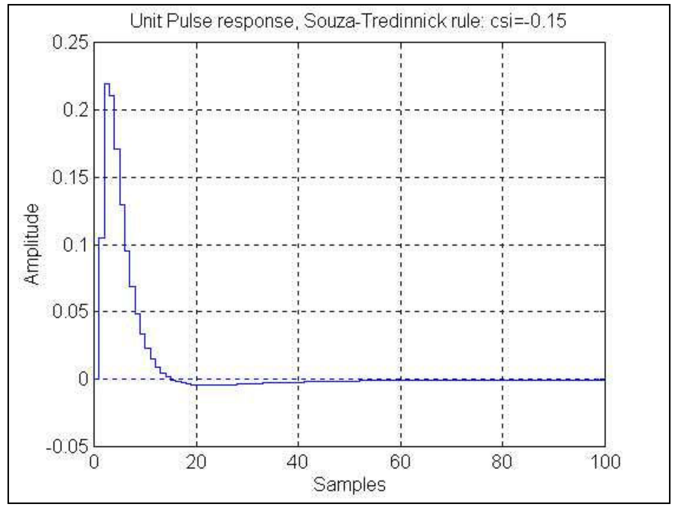

Fig.22. Vertical displacement response due a unit pulse input, with a PD controller designed by a ST1 rule.

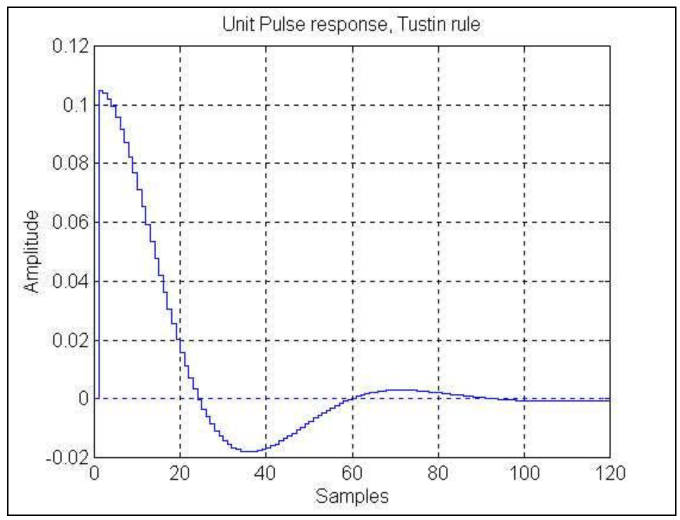

Fig. 23. Vertical displacement response due a unit pulse input, with a PD controller designed by a Bilinear rule.

10. Conclusions

In this work we tried some classical methods to preserve the stability of a flexible plant controlled by a discrete PD controller, but they all fail for a growing sample period. We also tried the Schneider mapping 1, and we showed that it fails for the PD controller and for any controller with derivative action. Then we proposed a new s-z mapping. The analysis and simulations so far suggest that this s-z mapping preserves the stability and improves it better than all other methods tried.

11. References.

Inman, D.J. *Engineering Vibration.* New Jersey: Prentice-Hall. 1996. 560 p.

Craig, R. R. *Structural dynamics: an introduction to computer methods*. New-York: John Wiley, 1981. 527p.

Deets, D.A.; Szalai, K.J. *Design and flight experience with a digital fly-by-wire control system using Apollo guidance system hardware on an F-8 aircraft*. Stanford: NASA. Flight Research Center, 1972. 12p. (AIAA paper 72-881).

Franklin, G.F.; Powell, D. *Digital control of dynamic systems*. Reading: Addison-Wesley, 1981. 335p.

Huntress, W.T. *Nasa's space science program: our outlook for the new millenium*. In: AAS – Strengthening Cooperation in the 21st Century, San Diego, 1996. Anais. EUA: San Diego, 1996; p.3-30.

Junkins, J.L.; Kim, Y. *Introduction to dynamics and control of flexible structures*. Washington: AIAA, 1993. 444p. (AIAA Educational Series).

Katz, P. ; Powell, J.D. *Sample rate selection for aircraft digital control*. AIAA Journal, v.13, n.8, p.975-979, Aug. 1975.

Meirovitch, L. *Methods of analytical dynamics*. New-York: McGraw-Hill, 1970b. 524p.

Ogata, K. *Engenharia de controle moderno*. Rio de Janeiro: Prentice-Hall, 1993. 773p.

Schneider, A.M.; Anuskiewicz, J.A.; Barghouti, I.S. *Accuracy and stability of discrete-time filters generated by high-order s-to-z mapping functions*. IEEE Transactions on Automatic Control, v.39, n.2, p.435-441, Feb. 1994.

Schneider, A. M.; Kaneshige, J. T.; Groutage, F. D. *Higher order s-to-z mapping functions and their applications in digitizing continuous-time filters*. Proceedings of the IEEE, v.79, n.11, p.1661-1674, Nov. 1991.

Schneider, A. M.; Groutage, F. D.; Volfson, L. B. *S-plane to z-plane mapping using a simultaneous equation algorithm based on the bilinear transformation*. IEEE Transactions on Automatic Control, v.AC-32, n.7, p.635-637, July 1987.

Tredinnick, M.R.A.C. *Controle Discreto da Atitude de Satélites Artificiais com Apêndices Flexíveis*. INPE – National Institute for Space Research. (Master thesis). São José dos Campos, Brasil. Feb. 26, 1999a (INPE-7179-TDI/680).

Tredinnick, M.R.A.C.; Souza, M.L.O.; Souza; L.C.G. 14th International Symposium on Space Flight Dynamics: *Digital Control of Artificial Satellites with Flexible Appendages*. Foz de Iguaçú, Pr, Brasil. Feb. 8-12, 1999b.